DOI: 10.1109/SEGE.2016.7589511

URL: http://ieeexplore.ieee.org/stamp/stamp.jsp?arnumber=7589511

Thomas Geury, Sonia Pinto and Johan Gyselinck
INESC-ID, Instituto Superior Técnico, University of Lisbon
BEAMS Energy, École polytechnique de Bruxelles, Université Libre de Bruxelles
Avenue Franklin Roosevelt 50 (CP165/52)
B-1050 Brussels
Belgium

Phone: +32 (0) 2 650 26 61
Fax: +32 (0) 2 650 26 53
Email: thomas.geury@ulb.ac.be

Direct Control Method for a PV System Integrated in an Indirect Matrix Converter-Based UPQC

Thomas Geury
F.R.I.A. scholarship student
INESC-ID, Instituto Superior T ´ecnico
BEAMS Energy, ´Ecole polytechnique de Bruxelles
Email: thomas.geury@ulb.ac.be

Sonia Pinto
INESC-ID Lisboa
Instituto Superior T ´ecnico
University of Lisbon
Lisbon, Portugal

Johan Gyselinck
BEAMS Energy
Ecole polytechnique de Bruxelles
Universit ´e Libre de Bruxelles
Brussels, Belgium

***Abstract*—This paper proposes a direct control method for a three-phase Photovoltaic (PV) system integrated on the Low-Voltage grid, using an Indirect Matrix Converter (IMC)-based Unified Power Quality Conditioner topology. This topology adds enhanced Power Quality functionality to the PV inverter when connected to a sensitive non-linear load, such as load current harmonics mitigation and voltage sags, swells and harmonics compensation. The PV array is inserted in the DC link of the IMC, which is controlled with a direct sliding mode control method. This direct control allows using a specific modulation method for the shunt converter that guarantees the DC link voltage is adequate for the operation of the IMC. Simulation results are presented to confirm the proper operation of the system under a variety of operating conditions.**

Keywords-photovoltaic systems; power quality; matrix converters; power harmonic filters; sliding mode control

I. Introduction

New challenges arise on the Low-Voltage (LV) grid due to the increasing use of distributed resources and power electronics-based equipment. Power Quality (PQ) issues such as voltage sags, swells and harmonics are of high concern when sensitive loads are connected to the grid. Also, the increasing use of non-linear loads, mainly power electronics-based equipment, results in low-order current harmonics which contribute to increasing losses and distorting the voltages in the Point of Common Coupling (PCC). In this context, active power filtering-based solutions have been proposed to improve PQ, either including series compensation, parallel compensation or both [1]–[3]. For distributed resources, new standards regarding the active voltage support are being developed.

Specifically, the connection of Photovoltaic (PV) systems to the LV grid is regulated by standards IEEE 1547, IEC 61727 and VDE 0126-1-1 (Germany), with particular attention to the current harmonics production (IEEE 61000-3-2) and the voltage quality with sags, swells and harmonics (EN 50160, Europe) [4]. In this context, the active support of the grid by distributed resources may be required (VDE-AR-N 4105, Germany), with voltage support in addition to the proposed current harmonics compensation in the point of connection to the grid or PCC [1], [5].

Depending on the grid characteristics, a shunt converter may be used for partially compensating both these current- and voltage-related issues [3]. However, in order to allow for a better voltage compensation, the system developed in this paper uses shunt and series converters for current and voltage compensation, respectively, forming a Unified Power Quality Conditioner (UPQC)-based topology [2], with a PV array inserted in the DC link [3], [6], [7]. An Indirect Matrix Converter (IMC) is used to form the UPQC, resulting in a direct connection between the equivalent shunt and series converters, without bulky DC-link storage capacitor, benefitting from the common advantages of Matrix Converters (MCs) [8].

This paper proposes a direct control method for the whole UPQC-based PV system, where sliding mode control is used for the shunt and series converters for current and voltage compensations, respectively. This contrasts with the non-direct control method developed in [6] and leads to a simpler implementation with faster control—the choice of the best control action is guaranteed regardless of the DC link variables. Still, a specific attention is paid to the modulation of the DC link voltage. Moreover, this topology has the advantage of acting as a step-up converter for the PV array voltage, removing the common DC/DC converter used at the PV array terminals, but the DC link voltage needs to be modulated for directly connecting the two converters and controlling the PV array and power flow to the grid at the same time.

II. Description of the PV System Topology

The UPQC-based topology proposed for the connection of the PV array to the LV grid is presented in Figure 1. The Voltage Source Converter (VSC) (or series converter) and the 3x2 MC (or shunt converter) form the IMC, with a direct connection through the DC link—which features switched current and voltage [9]—where the PV array is inserted using a filtering inductor L_{dc}.

The series converter is connected to the grid through a series transformer for compensating the voltage-related PQ issues, such as voltage sags, swells and harmonics [2], [10], in order to provide the sensitive load with adequate voltages $v_{\mathrm{nl,abc}}$ at the PCC. The compensation of the grid voltages v_{abc} by the series voltages v_{ABC} can be expressed by

$$v_{\mathrm{nl,abc}} = v_{\mathrm{abc}} - v_{\mathrm{ABC}}. \tag{1}$$

The shunt converter is connected at the PCC in parallel with the non-linear load for compensating its low-order current

978-1-5090-5110-6/16/$31.00 ©2016 IEEE

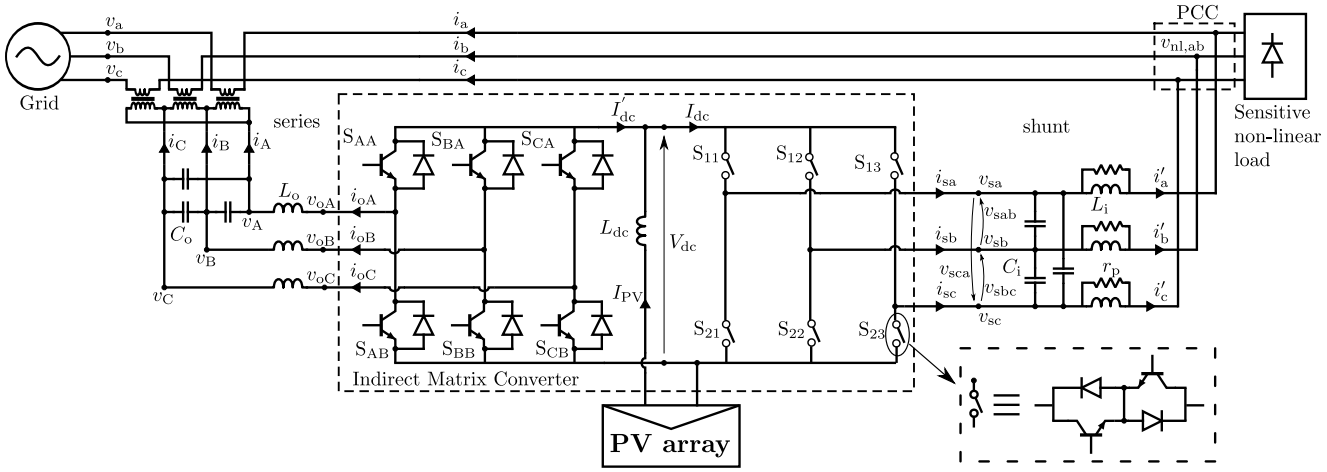

Figure 1. Detailed representation of the Indirect Matrix Converter-based Unified Power Quality Conditioner with the PV array inserted in the DC link

harmonics, and guaranteeing a nearly unitary Displacement Power Factor (DPF) at the point of connection to the grid. The compensation of the load currents $i_{\text{nl,abc}}$ by the shunt converter currents i'_{abc} can be expressed by

$$i_{\text{abc}} = i'_{\text{abc}} - i_{\text{nl,abc}}. \tag{2}$$

The IMC and its connection to the grid are detailed in Figure 1, with the relevant notations. It has the same number of switches (18 IGBTs and 18 diodes) and similar features to an MC; here, the shunt side is of the voltage-source type and the series side of the current-source type. However, a DC link is accessible for connecting the PV array due to the non-direct AC/AC conversion [8], [9], [11]. The converter can therefore be modelled as the combination of a 3x2 MC and a VSC.

The DC link voltage and current are determined by the 3x2 MC AC voltages and VSC AC currents, respectively. Thus, the VSC voltages v_{oABC} are obtained based on the 3x2 MC voltages v_{sabc} (3), and the 3x2 MC currents i_{sabc} are similarly obtained based on the VSC currents i_{oABC} (3).

$$\left[v_{\text{oABC}}\right] = \mathbf{S}_1\mathbf{S}_2^T\left[v_{\text{sabc}}\right], \quad \left[i_{\text{sabc}}\right] = \mathbf{S}_2\mathbf{S}_1^T\left[i_{\text{oABC}}\right] \tag{3}$$

$\mathbf{S}_1$ and $\mathbf{S}_2$ are the 3x2 MC and VSC switching matrices, respectively:

$$\mathbf{S}_1 = \begin{bmatrix} S_{11} & S_{12} & S_{13} \\ S_{21} & S_{22} & S_{23} \end{bmatrix}, \quad \mathbf{S}_2 = \begin{bmatrix} S_{\text{AA}} & S_{\text{AB}} & S_{\text{AC}} \\ S_{\text{BA}} & S_{\text{BB}} & S_{\text{BC}} \end{bmatrix}, \tag{4}$$

where the states $S_{kj}, \quad k \in \{1,2\},\ j \in \{1,2,3\}$ of the 3x2 MC switches and the states $S_{kj}, \quad k \in \{\text{A,B}\},\ j \in \{\text{A,B,C}\}$ of the VSC switches (1 when closed and 0 when open) must meet the common conditions $\sum_{j=1}^{3} S_{kj} = 1, \quad k \in \{1,2\}$ and $\sum_{k=\text{A}}^{\text{B}} S_{kj} = 1, \quad j \in \{\text{A,B,C}\}$, respectively.

The grid voltage sources are considered ideal with

$$v_k = \sqrt{2}V_{\text{rms}}\cos\left(\rho_v - (i-1)\frac{2\pi}{3}\right), \tag{5}$$

where $\rho_v = \omega t + \phi_v$ is determined by their constant pulsation ω and reference phase angle ϕ_v and $(k,i) = \{(\text{a},1),(\text{b},2),(\text{c},3)\}$. The system variables will be represented as space vectors in the two-axis non-rotating $\alpha\beta$ frame, using the power-invariant Concordia transform, and in the rotating dq frame, using the Concordia-Park transform. The latter is considered synchronous with the grid voltages ($\rho = \rho_v$ in the transform and $\phi_v = 0°$), such that the instantaneous power $p(t)$ and reactive power $q(t)$ are given by

$$\begin{aligned} p(t) &= v_d i_d \\ q(t) &= -v_d i_q \end{aligned}. \tag{6}$$

The dynamics of the shunt- and series-side filters will be detailed when developing the controllers of the converter.

III. Modulation of the Indirect Matrix Converter DC Link Voltage

The modulation of the DC link voltage is essential as it is used at the input of the series converter, for controlling the PV array current and for controlling the amplitude of the grid currents through the modulation of the shunt converter. The instantaneous DC link voltage has to meet two conditions: it must be equal to or higher than zero for the proper operation of the series converter and it must be equal to zero at some point for the proper control of the PV array current (see Section IV-C).

A specific modulation method is proposed here for the shunt converter in order to allow for the control of the d and q components of the grid currents while meeting the abovementioned conditions on the DC link voltage.

The switching states of the shunt converter are presented in Table I, based on the notations in Figure 1. The space current vectors corresponding to each of the switching states are represented in Figure 2a in the $\alpha\beta$ frame, where different zones corresponding to the location of the d component of the synchronously rotating dq frame are also specified. These are defined in Figure 3 in function of the grid line-to-line voltages.

The space vectors that are allowed for selection are a function of the zone considered. Considering the more common decomposition in 6 voltage zones delimited by the 6 non-

Figure 3 [1], only 2 non-zero space vectors can be applied per zone in order to guarantee a positive DC link voltage. For example, in the time interval between $T/4$ and $5T/12$ in Figure 3, considering the grid period T, or in the zone between vectors 2 and 3 in Figure 2a, voltages v_{bc} and $-v_{\text{ab}}$ should be applied to guarantee a positive DC link voltage. According to Table I, this corresponds to applying the space vectors 2 and 3. They would have to be applied alternatively with a zero vector in order to meet the two conditions and the control of the grid currents would determine which vector to apply: the d component would be increased by both non-zero vectors and the q component would be increased by vector 3 and decreased by vector 2. This is true as long as the projection of the space vector 3 on the q axis $\overrightarrow{3_q}$ is larger than the q component of the actual converter output current vector $\overrightarrow{i_{\text{s}q}}$, considering it is positive due to the reactive power consumption of the filter capacitors. However, as shown in the example in Figure 2b, this is usually not the case close to the edges of the zones where a third vector could be considered for optimizing the grid currents control—vector 4 could be considered for increasing i_q in this case as its projection on the q axis $\overrightarrow{4_q}$ is larger than $\overrightarrow{i_{\text{s}q}}$.

The consideration of a third non-zero vector does not interfere with the positive DC link voltage condition as long as the d axis is located close to the edge of one of the 6 zones, i.e. close to the full lines in Figure 3. Thus, it is here proposed to decompose the period in 12 zones instead, as shown in Figure 2a and Figure 3 with the dashed lines: only the two closest vectors are considered in the middle of the initial 6 zones (odd zones) but three vectors are considered in the zones around the edges (even zones) where they are guaranteed to result in a positive DC link voltage. This results in the vectors in Table II that meet the two conditions on the voltage and offer more possibilities for the control of the grid currents. In the example in Figure 2b, the use of vector 4 is enabled by the location of the d axis in zone 6.

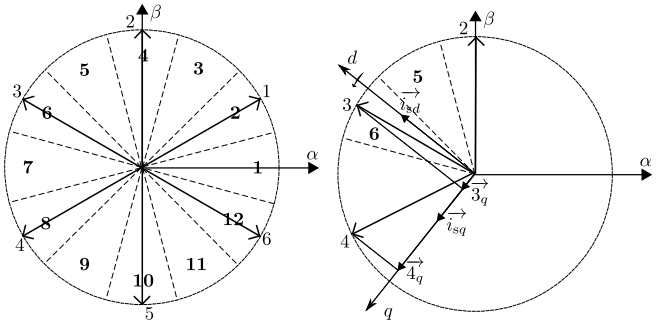

(a) All vectors and zones (b) Vectors to apply in zone 6

Figure 2. Current space vectors of the shunt converter with 12 zones (dashed lines)

IV. Direct Control of the Unified Power Quality Conditioner-Based PV System

The control of the system can be divided into three main objectives: controlling the grid currents to be sinusoidal

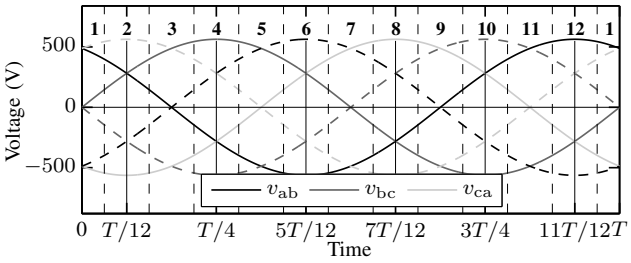

Figure 3. Decomposition of the grid period in 12 (dashed vertical lines) and 6 (full vertical lines) zones in function of the line-to-line grid voltages full lines) and their opposite (dashed lines).

TABLE I. Switching states of the shunt converter with the switches conducting on the upper **(1)** and lower **(2)** branches, with their effect on DC link voltage and AC currents

S	**(1)**	**(2)**	V_{dc}	i_{sa}	i_{sb}	i_{sc}	$\|\|\overrightarrow{i_{\text{s}}}\|\|$	$\arg(\overrightarrow{i_{\text{s}}})$
1	S_{11}	S_{23}	$-v_{\text{sca}}$	I_{dc}	0	$-I_{\text{dc}}$	$\sqrt{2}I_{\text{dc}}$	$\pi/6$
2	S_{12}	S_{23}	v_{sbc}	0	I_{dc}	$-I_{\text{dc}}$	$\sqrt{2}I_{\text{dc}}$	$\pi/2$
3	S_{12}	S_{21}	$-v_{\text{sab}}$	$-I_{\text{dc}}$	I_{dc}	0	$\sqrt{2}I_{\text{dc}}$	$5\pi/6$
4	S_{13}	S_{21}	v_{sca}	$-I_{\text{dc}}$	0	I_{dc}	$\sqrt{2}I_{\text{dc}}$	$-5\pi/6$
5	S_{13}	S_{22}	$-v_{\text{sbc}}$	0	$-I_{\text{dc}}$	I_{dc}	$\sqrt{2}I_{\text{dc}}$	$-\pi/2$
6	S_{11}	S_{22}	v_{sab}	I_{dc}	$-I_{\text{dc}}$	0	$\sqrt{2}I_{\text{dc}}$	$-\pi/6$
7	S_{11}	S_{21}	0	0	0	0	0	–
8	S_{12}	S_{22}	0	0	0	0	0	–
9	S_{13}	S_{23}	0	0	0	0	0	–

TABLE II. Non-zero switching vectors of the shunt converter that can be applied in function of the voltage zone considered

Zone	**1**	**2**	**3**	**4**	**5**	**6**	**7**	**8**	**9**	**10**	**11**	**12**
Vectors	1,6	1,2,6	1,2	1,2,3	2,3	2,3,4	3,4	3,4,5	4,5	4,5,6	5,6	5,6,1

through the current harmonics compensation of the shunt converter, controlling the voltages at the PCC through the series transformer voltage compensation of the series converter and controlling the PV array current to guarantee the proper power flow of the system through the generation of the grid current reference. Also, the PV array current reference can be generated so as to perform Maximum Power Point Tracking (MPPT). The control circuit is shown in Figure 4 where a direct sliding mode control method is used for both converters [10], [12] and generates the switching matrices $\mathbf{S}_1$ and $\mathbf{S}_2$ to apply to the shunt and series converters, respectively.

A. Sliding mode control of the shunt converter

The control of the shunt converter is based on the modulation of the DC link voltage described in Section III. The control laws for the power converter will be provided through discrete variables S_D and S_Q, corresponding to the respective control of the grid currents in the dq

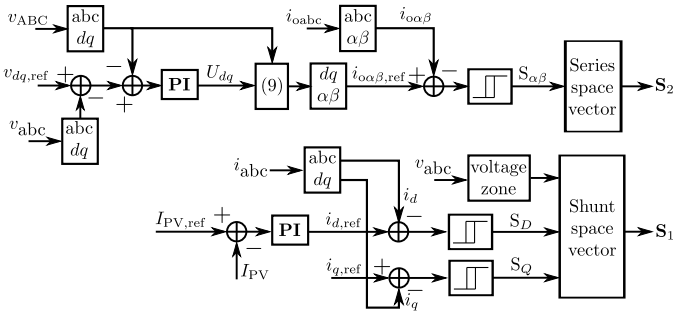

Figure 4. Control circuit of the shunt and series converters

TABLE III. SWITCHING VECTOR SELECTION FOR THE SHUNT CONVERTER IN FUNCTION OF THE VOLTAGE ZONE AND THE SLIDING VARIABLES

	Zone	1	2	3	4	5	6	7	8	9	10	11	12
$\{S_D,S_Q\}$	**{0,0}**	7	7	7	7	7	7	7	7	7	7	7	7
	{0,1}	7	7	7	7	7	7	7	7	7	7	7	7
	{0,2}	7	7	7	7	7	7	7	7	7	7	7	7
	{2,0}	6	6	1	1	2	2	3	3	4	4	5	5
	{2,1}	1	1	2	2	3	3	4	4	5	5	6	6
	{2,2}	1	2	2	3	3	4	4	5	5	6	6	1

the necessary information for choosing the most adequate switching state among the possibilities in Table II.

Considering the second-order grid-side filter, first-order sliding surfaces should be used for i_d and i_q [1], [12]:

$$S_{DQ}(e,t) = K_0\left(i_{dq,\text{ref}} - i_{dq}\right) + K_1\frac{\mathrm{d}}{\mathrm{d}t}\left(i_{dq,\text{ref}} - i_{dq}\right), \quad (7)$$

where K_0 and K_1 are positive-valued adjustable gains that affect the switching frequency of the converter, $e(t) = i_{\text{ref}} - i$ is the current error, and i_{dq} corresponds to the d and q components of the grid currents.

In order to guarantee a nearly unitary DPF, the reference for the q component of the grid currents is set to $i_{q,\text{ref}} = 0$. The current harmonics mitigation will be guaranteed by following a constant reference for the d component of the grid currents, whose actual value will result from the control of the PV array and the instantaneous power it generates.

According to [1], the shunt converter output currents i_{sd} and i_{sq} should be applied adequately to modify the time derivative of the sliding surfaces and help meeting the stability criterion $S(e,t)\dot{S}(e,t) < 0$, based on three- and two-level hysteresis comparators for i_d and i_q, respectively:

- If $S_{DQ}(e,t) < 0$ then $\mathrm{S}_{DQ} = 0$ and $\dot{S}_{DQ}(e,t) > 0$ is needed: i_{sdq} should be decreased
- If $S_D(e,t) \simeq 0$ then $\mathrm{S}_D = 1$ and $\dot{S}_D(e,t)$ should not be significantly modified: i_{sd} should not be modified in average
- If $S_{DQ}(e,t) > 0$ then $\mathrm{S}_{DQ} = 2$ and $\dot{S}_{DQ}(e,t) < 0$ is needed: i_{sdq} should be increased

Considering the available vectors in Table II, the selection of the switching vector to apply to the shunt converter in function of the voltage zone and the sliding surfaces is based on Table III. As mentioned in Section III, decreasing i_d is only possible using zero vectors.

B. Sliding mode control of the series converter

The series converter aims at producing the adequate voltages v_{ABC} at the series transformer ends, across the capacitors C_0. These voltages are governed by

$$C_{\text{o}}\frac{\mathrm{d}v_{\text{ABC}}}{\mathrm{d}t} = i_{\text{ABC}} - i_{\text{oABC}}. \quad (8)$$

After transformation, the converter output currents can be expressed in the dq frame with

$$\begin{aligned} i_{od} &= U_d + \frac{3}{2\sqrt{3}}C_{\text{o}}\omega v_d - \frac{3}{2}C_{\text{o}}\omega v_q \\ i_{oq} &= U_q + \frac{3}{2}C_{\text{o}}\omega v_d + \frac{3}{2\sqrt{3}}C_{\text{o}}\omega v_q \end{aligned}, \quad (9)$$

where the variables U_d and U_q result from the Proportional-Integral (PI) control of the series voltages, as shown in the control circuit in Figure 4 [13]. The converter output current references are then used for sliding mode control, based on the filter equation:

$$L_{\text{o}}\frac{\mathrm{d}i_{\text{oABC}}}{\mathrm{d}t} = v_{\text{oABC}} - v_{\text{ABC}}, \quad (10)$$

which can also be expressed in the $\alpha\beta$ frame by

$$L_{\text{o}}\frac{\mathrm{d}i_{o\alpha\beta}}{\mathrm{d}t} = v_{o\alpha\beta} - v_{\alpha\beta}, \quad (11)$$

These first-order dynamics lead to zero-order sliding surfaces:

$$S_{\alpha\beta}(e,t) = K_2\left(i_{o\alpha\beta,\text{ref}} - i_{o\alpha\beta}\right), \quad (12)$$

where K_2 is a positive-valued adjustable gain and $i_{o\alpha\beta}$ corresponds to the $\alpha\beta$ components of the converter output currents.

The current references are obtained from (9) considering $v_d = \sqrt{3}V_{\text{rms}}$ and $v_q = 0$ for balanced sinusoidal grid voltages as defined in (5). The switching states of the series converter are detailed in Table IV and the resulting output voltage vectors are represented in Figure 5 in the $\alpha\beta$ frame. Considering the dynamics in (11), the controlled currents $i_{o\alpha}$ and $i_{o\beta}$ are increased when the α and β components of the output voltage vector in Figure 5 are increased, respectively, and vice versa. This leads to the switching vector selection in Table V in function of the sliding surfaces.

C. PV array control

The use of zero vectors in the modulation of the DC link voltage allows controlling the PV array current I_{PV} with

$$V_{\text{PV}} - V_{\text{dc}} = L_{\text{dc}}\frac{\mathrm{d}I_{\text{PV}}}{\mathrm{d}t}. \quad (13)$$

The condition $V_{\text{dc}} < V_{\text{PV}}$ used to increase I_{PV} is met by applying zero vectors. In order to meet the condition $V_{\text{dc}} > V_{\text{PV}}$ used to decrease I_{PV} we need to guarantee that the DC link voltage

TABLE IV. SWITCHING STATES OF THE SERIES CONVERTER WITH THE SWITCHES CONDUCTING ON THE FIRST **(1)**, SECOND **(2)** AND THIRD **(3)** LEGS, WITH THEIR EFFECT ON DC LINK CURRENT AND AC VOLTAGES

S	**(1)**	**(2)**	**(3)**	$I_{\mathrm{dc}}^{'}$	v_{oAB}	v_{oBC}	v_{oCA}	$\|\overrightarrow{v_{\mathrm{o}}}\|$	$\arg(\overrightarrow{v_{\mathrm{o}}})$
1	S_{AA}	S_{BB}	S_{CB}	$-i_{\mathrm{A}}$	V_{dc}	0	$-V_{\mathrm{dc}}$	$\sqrt{2/3}V_{\mathrm{dc}}$	0
2	S_{AA}	S_{BA}	S_{CB}	i_{C}	0	V_{dc}	$-V_{\mathrm{dc}}$	$\sqrt{2/3}V_{\mathrm{dc}}$	$\pi/3$
3	S_{AB}	S_{BA}	S_{CB}	i_{B}	$-V_{\mathrm{dc}}$	V_{dc}	0	$\sqrt{2/3}V_{\mathrm{dc}}$	$2\pi/3$
4	S_{AB}	S_{BA}	S_{CA}	$-i_{\mathrm{A}}$	$-V_{\mathrm{dc}}$	0	V_{dc}	$\sqrt{2/3}V_{\mathrm{dc}}$	π
5	S_{AB}	S_{BB}	S_{CA}	i_{C}	0	$-V_{\mathrm{dc}}$	V_{dc}	$\sqrt{2/3}V_{\mathrm{dc}}$	$-2\pi/3$
6	S_{AA}	S_{BB}	S_{CA}	i_{B}	V_{dc}	$-V_{\mathrm{dc}}$	0	$\sqrt{2/3}V_{\mathrm{dc}}$	$-\pi/3$
7	S_{AA}	S_{BA}	S_{CA}	0	0	0	0	0	–
8	S_{AB}	S_{BB}	S_{CB}	0	0	0	0	0	–

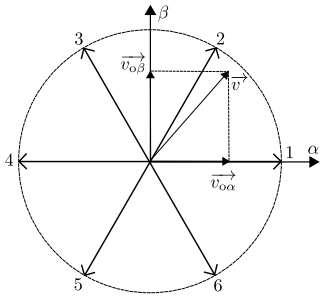

Figure 5. Voltage space vectors of the series converter in the $\alpha\beta$ frame

TABLE V. SWITCHING VECTOR SELECTION FOR THE SERIES CONVERTER IN FUNCTION OF THE SLIDING VARIABLES

S_α	**0**			**1**			**2**		
S_β	**0**	**1**	**2**	**0**	**1**	**2**	**0**	**1**	**2**
Vector	4	7	3	5	7	2	6	7	1

is larger than the PV array voltage for any non-zero vector. As shown in the control circuit in Figure 4, the control of the PV array current generates the reference for the d component of the grid currents with the following dynamics: increasing I_{PV} results in increasing the on-time of the zero vectors, i.e. in decreasing the amplitude of the AC current vector, and vice versa [1].

V. SIMULATION RESULTS

The PV system developed in this paper is simulated in the MATLAB/Simulink environment, with the parameter values in Table VI. The series transformer turns ratio is 1:2 with the primary connected to the grid. The PV array operates at rated conditions, with $I_{\mathrm{PV}} = 65\,\mathrm{A}$ and $V_{\mathrm{PV}} = 231\,\mathrm{V}$. The grid currents obtained in these no-load conditions, with all the PV array power flowing to the grid, are shown in Figure 6 and have a Total Harmonic Distortion (THD) of $3.01\,\%$.

TABLE VI. SIMULATION PARAMETER VALUES

Symbol	**Description**	**Value**	**Units**
T_{s}	Sample time	16	µs
v	Grid phase rms voltage	230	V
f_{g}	Grid frequency	50	Hz
a	Series transformer turns ratio	1:2	-
P_{PV}	PV array nominal power	15	kW
L_{dc}	PV array output inductance	12	mH
C_{i}	Shunt filter line-to-line capacitance	10	µF
L_{i}	Shunt filter phase inductance	4	mH
r_{p}	Shunt filter parallel resistance	40	Ω
C_{o}	Series filter line-to-line capacitance	10	µF
L_{o}	Series filter phase inductance	4	mH

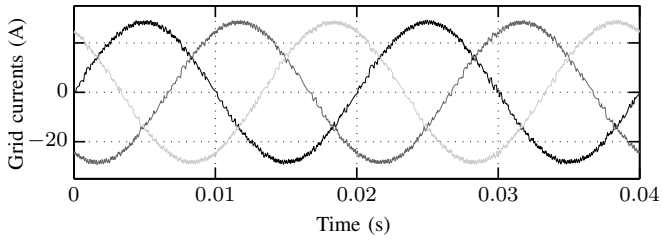

Figure 6. Grid currents in no-load operation – THD = $3.01\,\%$

In order to test the current harmonics compensation, a three-phase full-bridge diode rectifier non-linear load consuming a power of $5\,\mathrm{kW}$ is connected at the PCC. The currents consumed by the load are shown in Figure 7a with a THD of $22.38\,\%$ and particularly high 5^{th} and 7^{th} harmonics of $20.49\,\%$ and $7.6\,\%$ of the fundamental, respectively.

The currents inserted in the grid from the shunt converter (Figure 7b) compensate the load current harmonics such that the grid currents in Figure 7c have a THD of $4.78\,\%$, which is reduced to $2.45\,\%$ when considering only the first 40 harmonics (THD_{40}). Harmonics 5 and 7 are attenuated to $1.43\,\%$ and $1.87\,\%$ of the fundamental, respectively.

A phase grid voltage is presented in Figure 8 with a balanced $20\,\%$ sag in the grid voltages from $0.04\,\mathrm{s}$ to $0.16\,\mathrm{s}$ and then a $10\,\%$ swell from $0.24\,\mathrm{s}$ to $0.36\,\mathrm{s}$. The PCC or load phase voltage is shown in the same figure and keeps a constant amplitude thanks to the series voltage compensation. During the sag compensation, the PCC voltages have a THD of $1.96\,\%$ and the grid currents remain unaffected with a THD of $2.75\,\%$.

Realistic grid voltages are considered in Figure 9, where the phase grid voltage has 5^{th} and 7^{th} harmonics of $5\,\%$ and $3\,\%$ of the fundamental, respectively, and a THD of $5.83\,\%$. The harmonics are compensated by the series converter voltages to result in nearly sinusoidal PCC or load voltages with 5^{th} and 7^{th} harmonics of $1.27\,\%$ and $0.78\,\%$, respectively, and a THD of $2.55\,\%$.

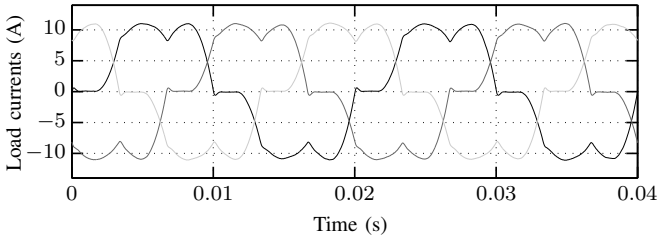

(a) Load currents – $\text{THD}_{40} = 22.25\,\%$

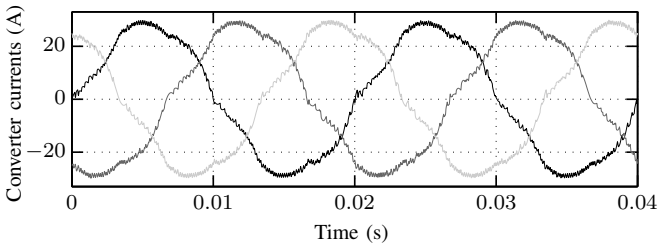

(b) Shunt converter AC currents – $\text{THD}_{40} = 7.93\,\%$

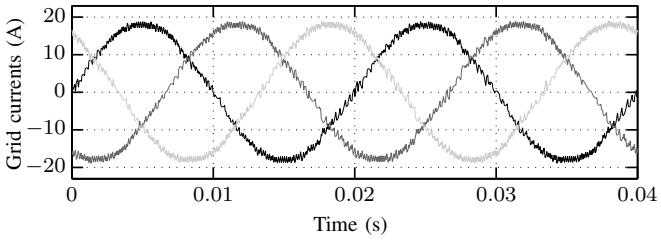

(c) Grid currents – $\text{THD}_{40} = 2.$

Figure 7. Current harmonics compensation of a 5 kW non-linear load

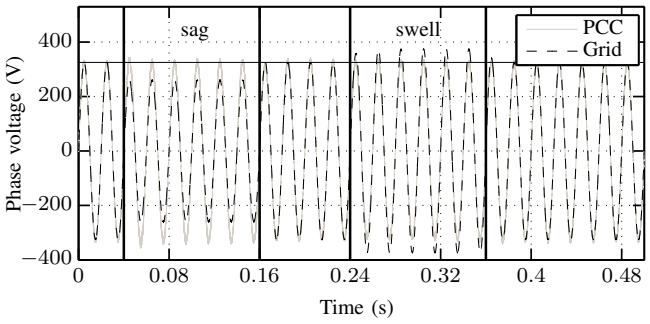

Figure 8. Compensation of voltage sags (from 0 04 s to 0 16 s) and swells (from 0.24 s to 0.36 s) – Phase grid (dashed line) and PCC (full grey line) with the amplitude reference (horizontal full line)

VI. Conclusion

A direct control method for a PV system integrated in a UPQC-based topology with the use of an IMC has been developed in this work. The availability of separate shunt and series converters allows mitigating both current- and voltage-related PQ issues with non-linear load current harmonics and voltage sags, swells and harmonics compensation for supplying sensitive loads. A specific modulation method is proposed for the shunt converter to properly control the DC link voltage, which is critical in this particular topology. That

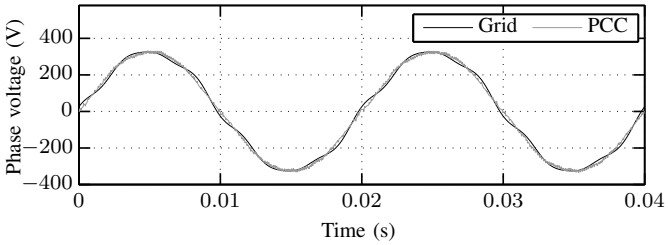

Figure 9. Compensation of voltage harmonics – Phase grid and PCC voltages

allows for direct sliding mode control of the whole IMC. Simulation results under these various abnormal conditions confirm the system operates properly.

Acknowledgment

Thomas Geury would like to thank the Belgian Fund for Research Training in Industry and Agriculture (FRIA) for the funding of this research project.

References

[1] T. Geury, S. Pinto, and J. Gyselinck, "Current source inverter-based photovoltaic system with enhanced active filtering functionalities," *IET Power Electronics*, vol. 8, no. 12, pp. 2483–2491, 2015.

[2] V. Khadkikar, "Enhancing electric power quality using UPQC: a comprehensive overview," *IEEE Transactions on Power Electronics*, vol. 27, pp. 2284–2297, 2012.

[3] Z. Zeng, H. Yang, S. Tang, and R. Zhao, "Objective-oriented power quality compensation of multifunctional grid-tied inverters and its application in microgrids," *IEEE Transactions on Power Electronics*, vol. 30, no. 3, pp. 1255–1265, 2015.

[4] R. Teodorescu, M. Liserre, and P. Rodriguez, *Grid converters for photovoltaic and wind power systems*. United Kingdom: John Wiley & Sons, Ltd., 2011.

[5] T. Geury, S. Pinto, and J. Gyselinck, "Three-phase Power Controlled PV Current Source Inverter with Incorporated Active Power Filtering," in *IECON 2013 - 39th Annual Conference of the IEEE Industrial Electronics Society*, 2013, pp. 1372–1377.

[6] T. Geury, S. Pinto, J. Gyselinck, and P. Wheeler, "An indirect matrix converter-based unified power quality conditioner for a PV inverter with enhanced power quality functionality," in *ISGT Asia - IEEE Innovative Smart Grid Technologies*. Bangkok: IEEE, 2015, pp. 1–8.

[7] K. Palanisamy, D. P. Kothari, M. K. Mishra, S. Meikandashivam, and I. Jacob Raglend, "Effective utilization of unified power quality conditioner for interconnecting PV modules with grid using power angle control method," *International Journal of Electrical Power and Energy Systems*, vol. 48, no. 1, pp. 131–138, 2013.

[8] J. W. Kolar, M. Baumann, F. Schafmeister, and H. Ertl, "Novel three-phase ac-dc-ac sparse matrix converter - Part I : Derivation, basic principle of operation, space vector modulation, dimensioning," in *Applied Power Electronics Conference and Exposition*, 2002, pp. 777–791.

[9] R. Peña, R. Cárdenas, E. Reyes, J. Clare, and P. Wheeler, "Control of a doubly fed induction generator via an indirect matrix converter with changing dc voltage," *IEEE Transactions on Industrial Electronics*, vol. 58, no. 10, pp. 4664–4674, 2011.

[10] S. Pinto, P. Alcaria, J. Monteiro, and J. F. Silva, "Matrix converter based active distribution transformer," *IEEE Transactions on Power Delivery*, 2016.

[11] J. Ferreira and S. Pinto, "P-Q decoupled control scheme for unified power flow controllers using sparse matrix converters," in *5th International Conference on the European Electricity Market*, May 2008, pp. 1–6.

[12] M. H. Rachid, *Power Electronics Handbook, Third Edition*. USA: Elsevier Inc., 2011, p. 1389.

[13] M. C. Cavalcanti, G. M. S. Azevedo, B. A. Amaral, and F. A. S. Neves, "Unified power quality conditioner in a grid connected photovoltaic system," *Electrical Power Quality and Utilisation, Journal*, vol. XII, no. 2, pp. 59–69, 2006.